

# Electron Diffraction from Graphene Starsmoke

NATHANIEL HUNTON

2003 Undergraduate Intern

Advisor: Dr. Phil Fraundorf

University of Missouri-St. Louis

## INTRODUCTION

This study attempts to compare various types of carbon found on Earth, with micron-sized spherical structures found in a meteorite that struck near Murchison, Australia in 1987 (Bernatowicz et al, 1996). The meteoritic spheres are referred to as onions because carbon atoms in their rims are organized in concentric graphitic shells, like the layers of an onion. Unlike terrestrial graphite onions (often called carbon blacks), the shells in these onions surround a core of randomly-oriented sheets of hexagonally-ordered graphene. When stacked in layers, such graphene sheets make up the graphite of pencils. Some of the atom-thick graphene sheets in the core of these onions appear to be bent into conical shapes by a pentagonal group of atoms (or some other defect) at the point of bending (Fraundorf and Wackenhut, 2002). Typical diameters of the onions themselves are between 0.5 and 2 microns (Bernatowicz et al, 1996). An image of one of these graphitic onions is shown in Fig. 1. Nanocones described in the core of one such onion are seen edge-on in Fig. 2.

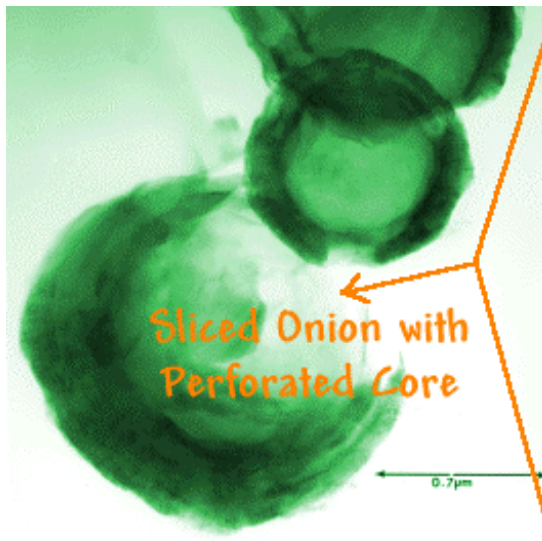


**Figure 1: Brightfield transmission electron microscope (TEM) image of presolar graphite onions with dark rims, and unlayered graphene cores, after sectioning and deposition on a holey carbon film. The perforated core region is an excellent location for high resolution imaging.**

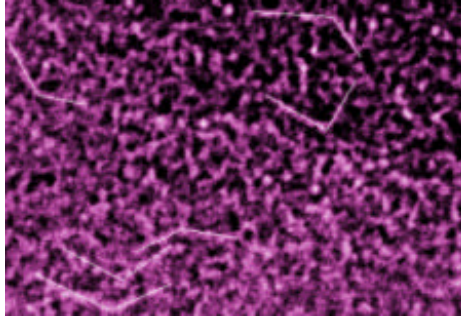


**Figure 2: Negative of a high resolution TEM image, in which several likely edge-on nanocones have been marked (from Fraundorf and Wackenhut, 2002). Field width is around 18 nm.**

These onions are of special interest because they are thought to originate in the outer atmospheres of red giant stars, or even in supernovae. The consensus that these grains are presolar stems from a study of the isotopic ratios for the atoms in the onions (Bernatowicz and Walker, 1997). In particular, the ratio of carbon-12 to carbon-13 does not match that for materials found on Earth (Bernatowicz et al, 1996). As a result, the abundances of atom-types in these grains provides information on nucleosynthesis (atom creation) that take place in the hot center of stars, as well as on processes which dredge up newly-created atoms into the star's atmosphere. The structure of these grains, in turn, provides information on processes of gas condensation which take place in stellar atmospheres and outflows, as well as on the nature and survival of dust in the interstellar medium. Interstellar dust, in turn, of course provides information on the material from which our solar system formed, including of course the primitive meteorites from which these particles were obtained. Finally, processes that make material rich in unlayered graphene are themselves of considerable interest in materials science. To date the only process for condensing graphene in almost totally unlayered form (e.g. as found in single-walled nanotubes) creates nanocones, but with much smaller cone angles than those discussed here (Kasuya et al, 2002).

## EXPERIMENTAL SETUP

A transmission electron microscope (TEM) was used for this study. In a TEM, an electron gun emits electrons; these electrons travel downward, passing through the specimen being examined. The electrons are scattered by the atoms in the sample, and sensors below the specimen detect these electrons and form an image from them.

A TEM has a special setting which can be used to create electron diffraction patterns of a sample. In the regular setting, the sensors are focused on the bottom of the specimen, where the electrons exit the sample, and record intensity as a function of vertical and horizontal position of incoming electrons. When a TEM is set up to create a diffraction pattern, the sensors are focused on the back focal plane, just below the specimen, and record intensity as a function of scattering angle and direction relative to the incident electron beam. Sometimes, in order to keep an especially intense center in a pattern from “drowning out” dimmer parts, a “beamstop”, which is a short, slender rod extending along a radius of the pattern, is used to block part of the center.

Electron diffraction patterns may be separated into two groups. In one group, the sample is a single crystal. These single-crystal diffraction patterns generally consist of spots in a geometric pattern, each corresponding to a set of atomic planes in the crystal which are scattering electrons strongly. Such a single-crystal pattern for silicon is shown below (Fig. 3).

The second type of electron diffraction, and the one used for this project, is called powder diffraction. The sample consists of many crystals that are oriented randomly, resulting in a sort of “powder”. This random orientation of numerous crystals causes the spots in the diffraction pattern to smear into concentric rings. Half of an experimental electron powder diffraction pattern for graphite is shown on the left half of (Fig. 4).

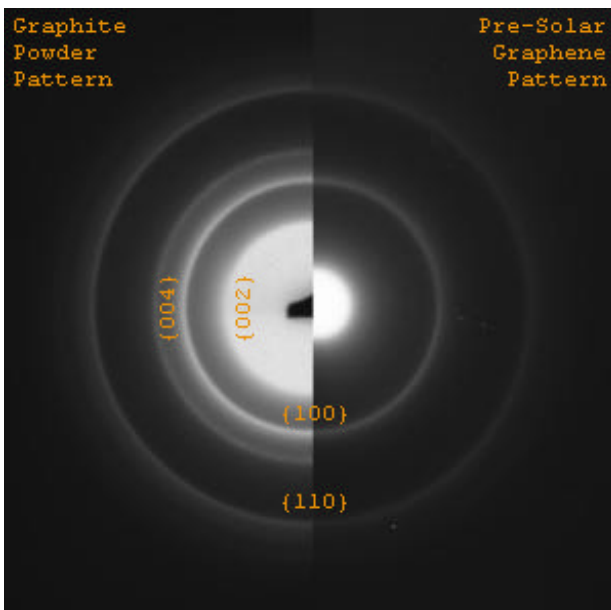


**Figure 4: Electron powder diffraction patterns - left half is terrestrial pyrolytic graphite; right half is graphene from the core of a presolar onion. Note the presence of only {hk0} spacings in the latter, showing the absence of graphite layering.**

#### Cores

The electron diffraction pattern from carbon in the core of a presolar graphite onion is shown on the right hand side of Figure 4. Note that any graphite rings not of the form {hk0} are missing in this pattern. This is evidence that the graphene sheets which make up this material have been assembled under conditions for which layering does not

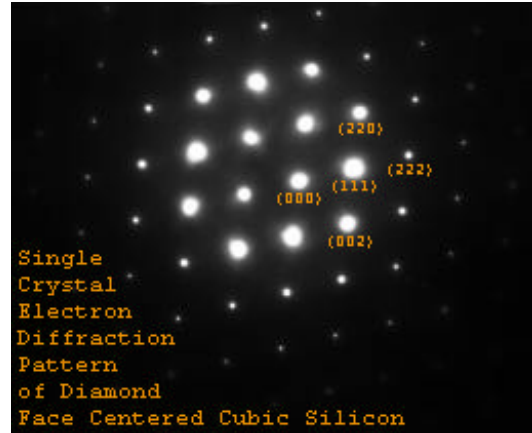


**Figure 3: Single crystal electron diffraction pattern of diamond face centered cubic silicon down a <110> direction.**

The electron powder diffraction patterns used for this study were quantitatively analyzed using the following process. Monotone negatives of the diffraction patterns were taken on transparent plastic film. Each negative was transferred to a computer using a scanner, and the resulting images were converted to 16-bit files. A program called Semper then recorded the average relative intensity of this image of the pattern as a function of distance from the pattern’s user-defined center. The resulting data was then inserted into a Microsoft Works file and a Mathematica file for graphing and analysis.

#### **OBSERVATIONS**

##### Diffraction from Presolar Graphite

occur. This is quite unusual, since even amorphous carbon often shows a diffuse {002} ring evidencing a tendency of the atoms to organize themselves in graphitic layers.

In Fig. 5 below, find an azimuthally-averaged intensity profile for the presolar onion electron-diffraction pattern in Figure 4. Intensity (on an arbitrary linear scale of 0 to 255) is plotted on the vertical axis, and distance from the pattern's center is plotted in inverse Angstroms on the horizontal axis. Note in particular the absence of the graphite {002} peak at 0.298 reciprocal Angstroms, and the asymmetry of the {hk0} diffraction peaks, which exhibit a more gradual decay on their high frequency side. This is

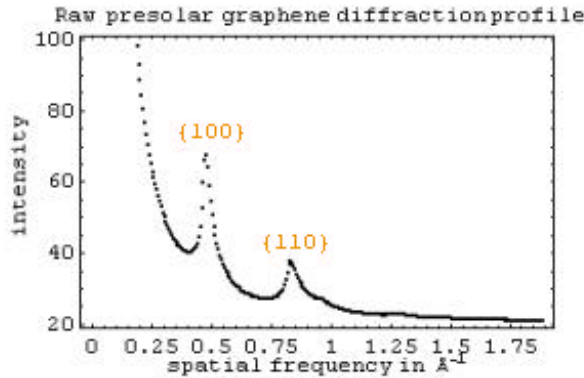


**Figure 5: Average greyvalue in the presolar graphene diffraction pattern of Fig. 4, as a function of radial distance from the center, or equivalently (thanks to the picometer wavelength of electrons being used) as a function of scattering angle or reciprocal lattice spacing in the specimen.**

independent evidence that the graphene sheets in the specimen are unlayered, i.e. only one atom thick.

Weaker peaks, which in graphite include weak (101) and (112) spacings, and in both graphite and unlayered graphene include the (200) spacing at 0.934 reciprocal Angstroms, will not be considered in more detail in the analysis to follow.

#### Observed Peak Shapes and their Meanings

To illustrate qualitatively what the "high frequency tails" in these diffraction rings mean, consider

Figure 6 below. This shows a simulated diffraction pattern, and high resolution TEM image, from a collection of randomly-oriented graphene sheets ranging in size from 3 to 40 Angstroms in size. The high frequency tails, quite well defined as "halos" around the

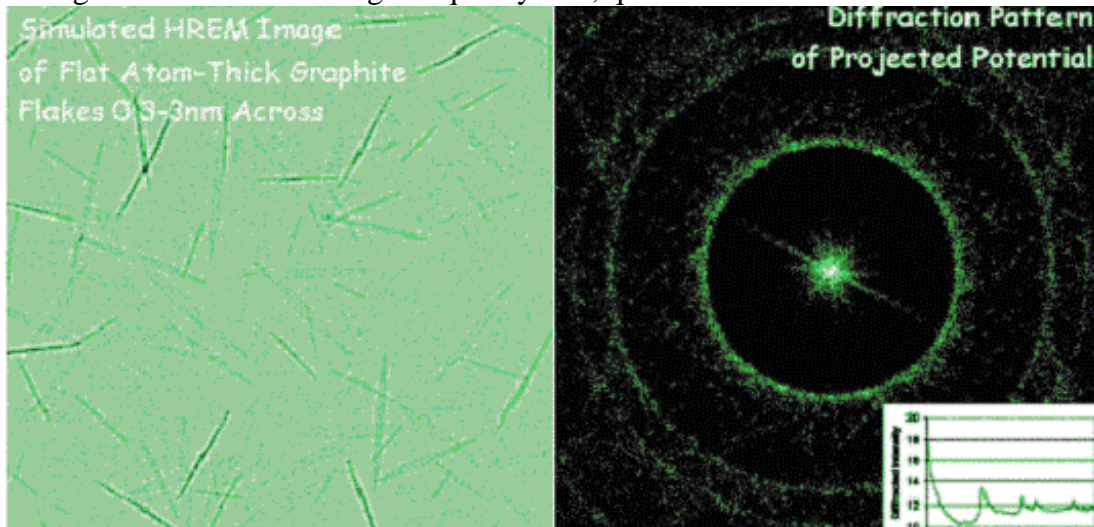


**Figure 6: Simulated high resolution TEM image and diffraction pattern from randomly oriented graphene sheets (Fraundorf et al, 2000).**

{100} and {110} diffraction rings, come from graphene sheets which are encountered by the electron beam at a non-zero angle to the sheet normal. These sheets are foreshortened, and thus appear to have a higher spatial frequency than they would have if encountered face on. The edge-on sheets (responsible mainly for radial streaks in the diffraction pattern) are the most obvious features in the high resolution image.

The details of these peak shapes have been of practical interest since the first half of last century (cf. Warren, 1941). The simplest possible model is perhaps to imagine a grating of spacing  $d$  and width  $w$  whose diffraction profile when encountered face on by the beam is a Gaussian profile at frequency  $1/d$  of full width half maximum  $1/w$ . If the width and spacing of the profile then change by ordinary geometric rules of foreshortening as the grating is tilted, then an average peak shape can be obtained by simply integrating this Gaussian over all possible orientations. An example is shown in Figure 7.

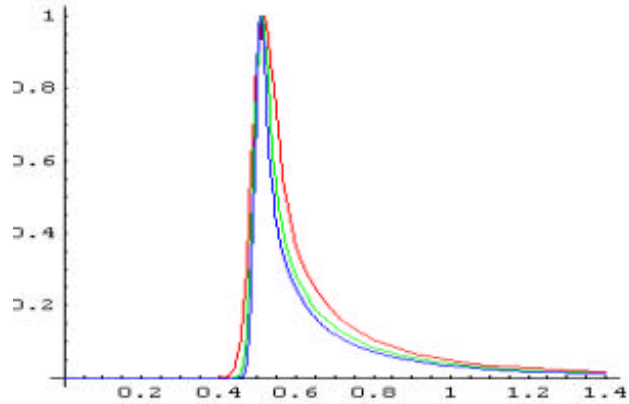


**Figure 7: Modeled powder diffraction profiles from graphene sheets of 40 (red), 60 (green), and 80 (blue) Angstroms width.**

Although this intensity distribution mimics the experimental peaks in its major features, the leading edge on the left side of the experimental peaks show more broadening than can be accounted for with a single size sheet (in agreement with

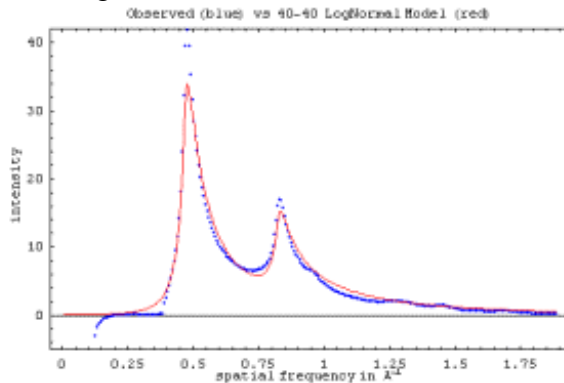


**Figure 8: Simulated diffraction profiles (red) from a log-normally distributed collection of randomly-oriented graphene sheets, having mean size and standard deviation of 40 Angstroms, compared to the experimental profile after background subtraction.**

observations of Bernatowicz et al, 1996). In fact, this broadening suggests (as we expect also from high resolution TEM images) that many of the graphene sheets are very small (e.g. 20 Angstroms in size or less). Log normal size distributions, very common among particulates found in nature, have this property of many more small than large. Therefore in Figure 8 we have used a log-normal distribution of sheet sizes (in this case with mean and standard deviations of 40 Angstroms each) to model both {100} and {110} graphene peak shapes. These simulated peaks are then compared to a background

subtracted version of the experimental profile. Although we have not yet optimized these parameters, the results suggest that a simple distribution of sheet sizes may be able to explain the diffraction data in detail.

## DISCUSSION AND CONCLUSIONS

Detailed study of electron diffraction profiles from the core of graphite onions formed in the neighborhood of asymptotic giant branch stars supports the existence of unlayered and randomly-oriented graphene sheets with mean size and standard deviation near 4 nm, likely with a size-distribution enriched in much smaller sheets. Future work will involve the optimizing of fit parameters, and possibly extension of the models to look for diffraction effects of pentagons in these hexagonally-coordinated sheets as well.

## REFERENCES

- Amari, S., Lewis, R.S., Anders, E. (1994). Interstellar Grains in Meteorites: I. Isolation of SiC, Graphite, and Diamond; Size Distributions of SiC and Graphite. Geochimica et Cosmochimica Acta, **58**, 459-70.
- Bernatowicz, T.J., Gibbons, P.C., Amari, S., Lewis, R.S. (1995). On the Nature of Carbon Cores in Interstellar Graphite. Lunar Planetary Science Conference XXVI.
- Bernatowicz, Thomas J., Cowsik, Ramanath, Gibbons, Patrick C., Lodders, Katharina, Fegley, Bruce, Jr., Amari, Sachiko, Lewis, Roy S. (1996). Constraints on Stellar Grain Formation from Presolar Graphite in the Murchison Meteorite. The Astrophysical Journal, **472**, 760-782.
- Bernatowicz, Thomas J., and Walker, Robert M. (1997). Ancient Stardust in the Laboratory. Physics Today, Dec. 1997, 26-32.
- Dawkins, D. (1996). Determination of the core to diameter ratio of interstellar dust particles from a carbonaceous meteorite. <http://newton.umsl.edu/~dawkins/grant.html>.
- Fraundorf, P., Brewer, K., Dawkins, D., Truong, M., Witt, D. (2000) The Core-rim Structure of Pre-solar Graphite Onions. Meteoritics and Planetary Science, **35**, 5, A56-57.
- Fraundorf, P. and Wackenhut, M. (2002) The core structure of pre-solar graphite onions, Astrophysical Journal Letters **578**, 2, L153-L156.
- Kasuya D., M. Yudasaka, K. Takahashi, F. Kokai and S. Iijima, J. Phys. Chem. B **106** (2002) 4947-4951
- Messenger, S., Amari, S., Gao, X., Walker, R.M., Clemett, S.J., Maechling, C.R., Chen, Y.H., Zare, R.N., Lewis, R. (1995). Organic Molecules in Interstellar Graphite Grains. Lunar Planetary Science Conference XXVI.
- Thomson, J.J. (1912). Further Experiments on Positive Rays. Phil. Mag., **24**, 209-253.
- Warren, B. E. (1941) X-ray Diffraction in Random Layer Lattices, Phys. Rev. **59** (9) 693-698.
- Zinner, E., Amari, S., Wopenka, B., Lewis, R.S. (1995). Interstellar Graphite in Meteorites: Isotopic Compositions And Structural Properties of Single Graphite Grains from Murchison. Meteoritics, **30**, 209-26.